First publ. in: The Journal of Immunology 173 (2004), 5, pp. 2762-2770

Specific Modulation of Astrocyte Inflammation by Inhibition of Mixed Lineage Kinases with CEP-1347166

Jeppe Falsig,*† Peter Pörzgen,* Julie Lotharius,* and Marcel Leist[2]*

Inflammator conversion of murineastrocytescorrelateswith the activation of various MAPK, and inhibition of terminal MAPKs like JNKorp38dampensthe inflammator reaction. Mixed lineagekinases(MLKs), a familyof MAPKkinase kinases,may therefore be involved in astrocyte inflammation In this study,weexploredthe effect of the MLK inhibitors CEP-1347 and CEP-11004 on the activation of murineastrocytesby either TNF plus IL-1or byacomplete cytokine mix containing additional IFN-γ. The compounds blockedNO-, PG-, and IL-6 release with a median inhibitory concentration of ~100 nM.Thisactivity correlated with a block of theJNKand the p38 pathways activated in complete cytokine mix-treated astrocytes. Although CEP-1347 did not affect the activation of NF-κB, it blocked the expression of cyclooxygenase-2 and inducible NO synthase at the transcriptional level. Quantitative transcript profilin of 17 inflammation-linke genes revealed aspecifi modulation patternof astrocyte activation byMLK inhibition,for instance, characterized by up-regulation of theanti-stress factorsinhibitor of apoptosis protein-2 and activated transcription factor 4, no effect on manganese superoxide dismutase and caspase-11, and down-regulation of major inflammator players like TNF,GM-CSF,urokinase-type plasminogen activator, and IL-6. In conclusion, MLK inhibitors likeCEP-1347 are highlypotentastrocyte immune modulators with a novelspectrum ofactivity.

Astrocytes, the most abundant celltypeintheCNS, are mainly responsible for CNS homeostasis. They alsotake part in the innate immune response ofthebrainand are capable of producing most inflammator mediators generally associated with macrophages, e.g., NO,PGs, ILs, chemokines, and extracellular proteases (1,2). Typical stimuli used to activateastrocytes are TNF-α, IL-1β, and IFN-γ (3) anda complete mixof these cytokinesresultsin afull-blown inflammatio response.

MAPKs playarole in theactivation of glia cells and regulate various inflammator endpoints. In brainautopsies,astrocytesdisplaying activated p38(4–6) and/orJNKcan befound in various pathological situations (7–10). In vitro JNK and p38are activated in astrocytes stimulated by proinflammator cytokines like IL-1β, and inhibition of JNKandp38 reduces expression ofinflammator endpoints like inducible NO synthase(iNOS),[3] TNF, and IL-6 (11). The expression patternofseveral MAPKssuggests involvement in various neurodegenerative diseases (12–14).

JNK and p38 are the convergence points of many physiological signals and acompletechronic blockade of these kinases might have unforeseen negative effects. Analternative strategy toblock only the pathologicalactivationof JNKand p38is to intervene at one of the controlling upstream kinases,such as the family of mixed lineagekinases(MLK).Therefore, we examined the role of MLKs in astrocyteinflammation

The MLKsare afamily ofserine/threonineMAPK kinase kinase (MAPKKK) (one among severalfamilies) involved in regulating signaling through the stress-activated protein kinases JNK and p38 (for a review, seeRef. 15). TheMLKscomprise a family of seven members and are typically activatedbyinflammator stimuli like LPS, cytokines, and stress. MLK3 is the best characterized of the MLKs. It has been shown that MLK3 (and other MLK family members)canactivate the JNK pathway through the phosphorylation of MAPK kinases (MKK) 4 and 7(16–19). Furthermore, MLK3 can phosphorylate MKK3, and thereby activate p38 (20).Most pharmacological workon MLKin mammalian cells is based on the use of the small-molecule inhibitor CEP-1347 (15). This compound is a semisyntheticderivative ofthe indolocarbazole K-252a with high selectivity for MLKs (21).

CEP-1347, which blocks all members of the MLK family, was discovered for its capacity to promote the survival of neurotrophin-deprived cholinergicneurons.Later, mechanistic studies showed that treatment with CEP-1347 selectively inhibits JNK activation induced by overexpression of different members of the MLKfamily (MLK1–3, dual leucinezipper-bearing kinase (DLK),leucine zipper-bearing kinase(LZK)),but not activationinduced by membersof other MAPKKK families like MAPK/ERK kinase 1, tumor progression locus 2, and apoptosissignal-regulating kinase1(22). CEP-1347 inhibits MLK family members bycompetingfor ATP binding.

CEP-1347 has an IC_{50} value of 60 nM for MLK1,80nM for MLK2, and 40 nM for MLK3inacell-based kinase assay, while it does not directly inhibit MKKs, JNK, or p38 in cells (22). CEP-11004 is a selective MLK inhibitor of the same structural class as CEP-1347. It is also neuroprotective in vitro as well as in vivo, and inhibits activation of JNKbyMLK in cells/tissue within aconcentration range of 30–1000 nM (23). The availability of specifi and cell-permeable MLK inhibitors allows the examination of the role of MLKs in astrocyteinflammation In this report, we examined whether MLK inhibition blocked the release of inflammator

*H. Lundbeck, Valby, Denmark; and †Department ofNeuropathology, Universityof Zürich, Zürich, Switzerland

Received for publication December 15, 2003. AcceptedforpublicationJune 10, 2004.

The costs of publication of this article were defrayed inpart by thepaymentof page charges. This article must therefore be hereby marked *advertisement* in accordance with 18 U.S.C. Section 1734 solely to indicate this fact.

[1] Financial disclosure: The authors are orhavebeenemployedatH.Lundbeck.The company is currently involvedinaclinicaltrial (PRECEPT) testingone of the model drugs used in this study(CEP-1347).

[2] Address correspondenceandreprint requests to Dr. Marcel Leist,Disease Biology, H. Lundbeck, Ottiliavej 9, 2500 Valby,Denmark. E-mail address: male@lundbeck.com

[3] Abbreviations used in this paper: iNOS, inducible NO synthase; MLK, mixedlineage kinase; MAPKKK,MAPK kinase kinase;MKK,MAPK kinase; CCM, complete cytokine mix; PBS-G,PBS with 2 g/L glucose; Cox-2, cyclooxygenase-2; GFAP, glial fibrillar acidic protein; Tc, threshold cycle; ATF4, activated transcription factor 4; IAP-2,inhibitor of apoptosis protein-2; uPA, urokinase-type plasminogen activator; MnSOD,manganese superoxidedismutase;DLK, dual leucinezipper-bearing kinase.

mediators and the activation of MAPK. We examined the correlation of these effects in astrocytes, and described a new pattern of inf ammatory modulation due to MLK inhibition.

Materials and Methods

Materials

Complete cytokine mix (CCM) contained 10 ng/ml murine TNF-α, 10 ng/ml murine IL-1β (Sigma-Aldrich, Copenhagen, Denmark), and 5 U/ml recombinant murine IFN-γ (R&D Systems, Abingdon, U.K.). Other reagents were CEP-1347 (3,9-Bis[(ethylthio)methyl]-K-252a) and CEP-11004 (3,9-Bis[(propylthio)methyl]-K-252a) (21) both synthesized at Cephalon (West Chester, PA) and Ono-2506 ((R)-(-)-2-propyloctanoic acid) (24) synthesized by H. Lundbeck (Valby, Denmark). Basic laboratory chemicals and inhibitors were purchased from Sigma-Aldrich unless stated otherwise.

Primary astrocyte cultures

Pregnant C57BL/6jbom mice were purchased from Harlan (Horst, Holland). All experimental procedures were conducted in accordance with the directives of the Danish National Committee on Animal Research Ethics and the European Communities Council Directive No. 86/609 for care of laboratory animals.

Primary cortical astrocytes were prepared from 1- to 2-day-old mice according to a slightly modif ed version of a protocol by Weinstein (25). In brief, brains from six pups were removed and kept on ice in a PBS buffer containing 2 g/L glucose and 0.001% (w/v) phenol red, pH 7.4 (PBS-G). The cortices were dissected out, and hippocampi and meninges were carefully removed before digestion in PBS-G containing 10 mg/ml trypsin TRL (Worthington Biochemical, Lakewood, NJ), 1 mg/ml DNase (Worthington Biochemical), and 5 mg/ml $MgSO_4$ for 3 min at 37°C. Tissue was washed in PBS-G and triturated in PBS-G with 0.5 mg/ml DNase using sequentially an 18-, 20-, and a 23-G needle. Cells were f ltered through a 70-μm mesh (Falcon; BD Biosciences, Brøndby, Denmark), pelleted (150 $\times$ *g* for 5 min), and resuspended in PBS-G containing DNase and $MgSO_4$. Cells were carefully layered over a 30% Percoll solution (Amersham Biosciences, Hørsholm, Denmark) in PBS-G and centrifuged at 150 $\times$ *g* for 10 min. Cells were recovered from the interface, washed once with 15 ml of PBS-G (100 $\times$ *g* for 5 min), and resuspended in DMEM (high glucose), 10% FCS, 100 U/ml penicillin, and 100 μg/ml streptomycin. This medium was used for growing cells, but for all experiments cells were changed into 2% FCS. All medium constituents were purchased from Invitrogen Life Technologies (Taastrup, Denmark). Cells were counted in a trypan blue solution to assess viability, and seeded at a density of 10,000 cells/cm^2 in 185 cm^2 f asks (all dishes used were from Nunc, Roskilde, Denmark). The medium was changed after 3 days, and subsequently twice a week. Cells were trypsinized and reseeded after 14 days in primary culture and were always used for experiments 6–8 days after replating.

Standard cell incubation scheme

CCM model. Cells were preincubated with inhibitors for 30 min before addition of cytokine mix (CCM). After 24 h, protein, cytokine production, and nitrite production were measured. For signaling studies, samples were lysed after 30–60 min. For time titration of mRNA or protein expression levels, CCM was added at different times. Cells and supernatant from all wells were then harvested at the same time.

Enzyme-linked immunoassays

IL-6 was measured using a murine-specif c OptEIA ELISA kit from BD Pharmingen (Brøndby, Denmark) in MaxiSorp plates from Nunc. PGE_2 was measured using a competitive immunoassay, correlate-EIA kit from Assay Designs (Ann Arbor, MI), according to the manufacturer's instruction. The kit has cross-reactivity to PGE_1 (70%) and PGE_3 (16.3%). RANTES was measured using the murine-specif c Quantikine M kit from R&D Systems.

Nitrite measurement

Nitrite was measured by use of the Griess reagent. In brief, 50 μl of supernatant or $NaNO_2$ standards were mixed with 25 μl of *N*-(1-naphthyl) ethylenediamine (0.1% in H_2O) and 25 μl of sulfanilamide (1% in 1.2N HCl) in a 96-well plate. After 3 min, samples were read at 570–690 nm.

Western analysis

The protein levels of cyclooxygenase-2 (Cox-2), iNOS, glial f brillary acidic protein (GFAP), and β-actin were assessed using Western blot analysis. Astrocytes were washed once in PBS before lysis in ice-cold buffer containing 1% Nonidet P-40, 20 mM Tris-HCl, pH 8.0, 137 mM NaCl, 10% glycerol, 4 mM iodo acetamide, 10 mM NaF, 1 mM 4-(2-aminoethyl)-benzene sulfonyl f uoride hydrochloric acid (AEBSF), 1 mM Na_3VO_4, and "Complete mini" protease-inhibitor mix from Roche (1 pill/10 ml buffer; Hvidovre, Denmark). The lysate was transferred to a microfuge tube and incubated for 15 min on ice before cellular debris was spun down for 10 min at 10,000 $\times$ *g*, 4°C. The supernatants were transferred to a fresh tube and stored at −80°C. The protein concentration was determined by the bicinchoninic acid method using a commercial kit from Pierce (Rockford, IL). The NuPAGE-kit (4–12% Bis-Tris gel run with MOPS buffer under reducing conditions) from (Invitrogen Life Technologies) was used for electrophoresis according to the manufacturer's instruction. Gels were run for ~1 h at 200 V before blotting proteins onto an activated PVDF membrane (Immobilon P; Millipore, Glostrup, Denmark) using wet-transfer blot module XCell2 from Invitrogen Life Technologies. Membranes were blocked with 5% milk in TBST (2.42 g/L Tris base, 8 g/L NaCl, and 0.1% Tween 20, pH 7.6), washed with TBST and incubated with primary Ab dissolved in 5% milk in TBST overnight at 4°C. Blots were washed and incubated with appropriate HRP-conjugated secondary Abs, (rabbit anti-mouse 1/2,000, and goat anti-rabbit 1/1,000 both from DAKO (Glostrup, Denmark)) for 1 h at room temperature, and developed using ECL or ECL+ (Amersham Biosciences). Primary Abs used were mouse IgG anti-GFAP clone G-A-5 (Sigma-Aldrich) used at a dilution of 1/1,000. Rabbit polyclonal anti-mouse Cox-2 (1/1,000) and rabbit polyclonal anti-mouse iNOS (1/2,000) from Alexis were purchased through A. H. Diagnostics (Aarhus, Denmark). Mouse anti-β-actin clone AC-15 (Sigma-Aldrich) (1/5,000) was also used.

For signaling studies, the same Western blot procedure was used. The membranes were f rst stained with a phosphospecif c Ab, stripped, and reblotted with the phospho- nonspecif c Ab or anti-β-actin. The membranes were sealed in a plastic bath with 10 ml of a stripping buffer (2% SDS, 50 mM Tris-HCL, and 100 mM 2-ME) and incubated for 25 min at 55°C in a water bath.

Primary Abs used were rabbit polyclonal anti-phospho-Akt at a dilution of 1/1,000, rabbit polyclonal anti-Akt (1/1,000), rabbit polyclonal anti-phospho-ERK (1/1,000), and rabbit polyclonal anti-c-Jun (1/2,000) all from Cell Signaling Technology (Beverly, MA), but purchased through Medinova Scientif c (Hellerup, Denmark). Mouse monoclonal anti-phospho-c-Jun clone KM-1 (1/1,000), mouse monoclonal anti-phospho-JNK clone F-7 (1/1,000), mouse monoclonal anti-phospho-MKK3/6 clone B-9 (1/500), rabbit monoclonal anti-MKK3 clone N-20 (1/1,000), and goat monoclonal anti-MKK6 clone V-20 were all purchased from Santa Cruz Biotechnology (Santa Cruz, CA).

Quantitative PCR

Cells stimulated in 10-cm dishes were washed once with PBS and total RNA was extracted using TRIzol reagent (Invitrogen Life Technologies) according to the manufacturer's protocol. Purif ed RNA was treated with DNA-free, DNase-1 (Ambion, Huntingdon, U.K.) according to the manufacturer's protocol. Total RNA (1 μg) was reverse transcribed with TaqMan RT Reagent (Applied Biosystems, Naerum, Denmark) using random hexamers in a 100-μl reaction on a PTC-200 DNA Engine Thermal Cycler (VWR International, Albertslund, Denmark), using a program of 10 min annealing at 25°C, 30-min reverse transcription at 48°C, 5-min inactivation at 95°C. The cDNA was quantif ed using the SYBR GREEN PCR Master Mix kit (Applied Biosystems). Each reaction contained 2.5 μl of cDNA of the 100-μl reverse transcription product, 300 nM forward and reverse primers, 12.5 μl of master mix, and 7 μl of water in a total volume of 25 μl. PCR amplif cation was run in a 96-well experimental plate format on an iCycler Thermal Cycler equipped with an iCycler Optical System (Bio-Rad, Hercules, CA). The program set-up was 10 min at 95°C, 40 cycles of 15′ at 95°C/1 min at 60°C. A melting curve was obtained to verify the measured signal and the product was run on a 4% agarose gel to verify the presence of only one band. Quantif cation was performed as follows: using the iCycler data analysis software (Bio-Rad), the threshold cycle (Tc) was determined for each sample. Tc was def ned as the cycle at which the level of f uorescence increased signif cantly above the background levels of f uorescence. The concentration of cDNA was calculated by comparing the Tc of samples to the Tc of a standard curve. The standard curve was obtained by a serial dilution of cDNA. Each sample was run in two reactions, one with the primer set of interest and one with a GAPDH primer set, and all data are displayed as the ratio between the calculated starting concentration of the cDNA of interest and GAPDH. All primers except for the housekeeping gene *GAPDH* were intron spanning to distinguish cDNA from genomic DNA. For GAPDH, the order of magnitude between the samples and the samples without reverse transcriptase was above 10^6. Primers used were GAPDH sense (Accession no. NM_008084): 5′-TGC ACC ACC

AAC TGC TTA G-3′, antisense: 5′-GGA TGC AGG GAT GAT GTT C-3′. Activated transcription factor 4 (ATF4) sense (NM_009716): 5′-CTC CTCGGCCCAAACCTTATGA-3′, antisense 5′-GGTACCTAGTGGCT GTCTTGTTTT-3′. Cox-2 sense (NM_011198): 5′-GTG TGA CTG TAC CCG GAC TGG ATT CTA-3′, antisense: 5′-ACT GTG TTT GGG GTG GGC TTC A-3′. DLK sense (NM_009582): 5′-CTT TGG GGG CTT TGT GTC TAC TCT AA-3′, antisense 5′-GTG GGC GTC AGG TCT TTC TCG-3′. Inhibitor of apoptosis protein-2 (IAP-2) sense (NM_007465): 5′-GTC TGG CTC GTG CTG GCT TTT ATT AT-3′, antisense 5′-TGT CCC CTT GTT TCC AGT TAT CCA-3′. IL-6 sense (J_03783): 5′-GGA GCC CAC CAA GAA CGA TAG TCA-3′, antisense: 5′-GAA GTA GGG AAG GCC GTG GTT-3′. iNOS sense (NM_010927): 5′-TTG CCA CGG ACG AGA CGG ATA GG-3′, antisense: 5′-GGG CAC ATG CAA GGA AGG GAA CTC-3′. MLK1 sense (NM_177395): 5′-CGC CTT CGA GCC ATC CAG TT-3′, antisense 5′-GCT CCG GCC CCA GGT TTT AC-3′. MLK2 sense (XM_194344): 5′-CGC CGC ACC CTC AGA CCT-3′, antisense 5′-CCA TAC GGC GCG ATA GAC TTT G-3′. MLK3 sense (NM_022012): 5′-TGT CTT GCC GTA GCC TAT GGT GTG-3′, antisense 5′-TGC GGT GGG GGT CCT GTG-3′. RANTES sense (NM_013653): 5′-GCA GCT GCC CTC ACC ATC ATC-3′, antisense 5′-GAG GCA GCG CGA GGG AGA G-3′. TNF sense (Accession no.: NM_013693): 5′-CTA TGG CCC AGA CCC TCA CAC TCA-3′, antisense: 5′-CAC TCC AGC TGC TCC TCC ACT TG-3′. Urokinase-type plasminogen activator (uPA) sense (NM_008873): 5′-AGG TTT ACT GAT GCT CCG TTT GGT TC-3′, antisense 5′-TTT ACG ACG GAC ATT TTC AGG TTC TTT-3′. Primers were designed using the DNAS TAR software package (Madison, WI) and all primers were blasted using BLASTn (www.ncbi.nlm.nih.gov/BLAST/).

Transcript analysis by oligonucleotide hybridization analysis

We selected a short list of mouse genes known to be up-regulated in astrocyte inf ammation. For each of these genes, one oligonucleotide (40–50 mer) was designed by MWG Biotec (Ebersberg, Germany) using their proprietary Oligo4array software and CodeSeq database, which selects the oligos preferentially from the 3′-region of each coding sequence. Furthermore, each oligomer was scrutinized to meet physicochemical parameters (like melting temperature, self-complementarity, secondary structure, etc.) and extensively tested to minimize cross-hybridization to other sequences of the mouse genome in silico. All oligos were synthesized using MWG Biotec's high purity salt-free technology followed by MALDI-TOF quality control.

The oligomers were spotted onto activated glass slides (Pan Epoxy, MWG Biotec or CodeLink, Amersham) using a 417 Affymetrix "ring and pin" spotter (purchased through MWG Biotec). Sample preparation and labeling was conducted as described by J. DeRisi (www.microarrays.org/protocols.html), a protocol derived from Hughes et al. (26). In brief: 12–15 μg of total RNA were reverse transcribed using a random hexamer and dT16 primers and Superscript II reverse transcriptase (Invitrogen Life Technologies), incorporating amino-allyl dUTP into the f rst strand cDNA. After the cDNA synthesis, the remaining RNA was hydrolyzed and after a clean-up step (Microcon-30 spin f lters; Millipore), Cy-3 or Cy-5 dye esters, respectively, were coupled to the cDNA samples. Excessive dye and buffer were removed with QiaQuick PCR purif cation columns (Qiagen, Valencia, CA) and the eluates were concentrated with Microcon-30 spin f lters. The hybridization mixture contained the Cy-labeled cDNAs in hybridization buffer (50% formamide, 6× SSC, 5× Denhardt's, 0.5% SDS, and 50 mM sodium phosphate, pH = 8) and was denatured for 5 min before incubation on the slides for 16 h at 42°C. Washing was conducted in three steps of increasing stringency: 2× SSC, 0.1% SDS followed by 1× SSC, 0.01% SDS and 0.5× SSC (all solutions were preheated to 30°C). Finally, each slide was spun dry and scanned in a 428 Affymetrix confocal laser scanner at three different intensities (photo multiplier gains).

The microarrays were analyzed using ImaGene 4.2 (BioDiscovery; purchased through MWG Biotec) for spot location, array alignment, and background subtraction. Signal intensities for individual spots were adjusted for local background. Microsoft Excel was used for further statistical analysis of the ImaGene output f les, e.g., Cy3-Cy5 ratio normalization was conducted by multiplying each ratio value with a scaling factor, which was def ned as the ratio of the overall signal intensity of the Cy5 vs Cy3 channel (27). Each microarray experiment was performed at least twice independently. To further account for bias introduced by dye bleaching or labeling, each experiment was conducted as a dye-swap experiment with the resulting ratio value being the arithmetical mean from two slides of opposite-labeled sample pairs. Genes with very low signal intensities (<5-fold of the background) were excluded from the analysis.

NF-κB assays

NF-κB p65 transcription factor assay TransAM from Active Motif (Rixensart, Belgium) was performed according to the manufacturer's protocol (28). In brief, cells were stimulated appropriately and lysed using the supplied lysis buffer mixed with DTT and protease inhibitors. The protein concentration was determined using the bicinchoninic acid method. An ELISA plate precoated with NF-κB consensus element (5′-GGGACTT TCC-3′) was blocked with herring sperm DNA and soluble wild-type consensus element was added to half of the wells to compete out the p65-binding. Twenty micrograms of protein of every sample were added to each of four wells, two wells with, and two wells without the competing oligonucleotide. The plate was incubated for 1 h and washed three times with the supplied wash buffer. A primary p65 Ab that recognizes an epitope, only accessible when p65 is bound to DNA was added and after shaking for 1 h the plate was washed three times. A secondary HRP-conjugated Ab was added and after 1 h the plate was washed four times and developing solution was applied. Ten minutes later, a stop solution was added and the absorbance was read at 450–690 nm using a spectrophotometer. Results displayed are the total signal for each sample minus the signal not competed out by the large excess of wild-type oligonucleotide.

NF-κB p65 translocation assay. Primary astrocytes were stimulated in 96-well plates and the Cellomics HitKit (Reading, U.K.) was used according to the manufacturer's protocol to stain the cells. In brief: cells were f xed, permeabilized, and subsequently stained with a primary Ab against the NF-κB p65 subunit. A secondary Alexa Fluor 488-conjugated secondary Ab was used as a detection Ab together with 5 μg/ml Hoechst 33342. The plate was loaded onto the Cellomics Arrayscan II system. Using the cytoplasm to nuclear translocation application, the system automatically located, focused, and exposed according to application-specif c criteria, and read and analyzed the images collected from multiple f uorescent channels. Changes in the distribution of f uorescently labeled NF-κB were automatically analyzed and quantif ed using image-based algorithms and exported to an Excel spreadsheet. An average of 90 cells per f eld and a total of 10 f elds per well were counted. Each data point is the average of three wells displayed as the total nuclear f uorescence (determined by colocalization with Hoechst 33342) minus the total cytoplasmic f uorescence.

p-c-Jun assay

p-c-Jun assay. Primary astrocytes were stimulated in 96-well plates and the Cellomics HitKit was used according to the manufacturer's protocol to stain the cells. In brief, cells were f xed, permeabilized, and subsequently stained with a primary Ab against the phosphorylated c-Jun. A secondary Alexa Fluor 488-conjugated secondary Ab was used as a detection Ab together with 5 μg/ml Hoechst 33342. The plate was loaded onto the Cellomics Arrayscan II system. Using the cytoplasm to nuclear translocation application, the system automatically located, focused, and exposed according to application-specif c criteria, and read and analyzed the images collected from multiple f uorescent channels. Changes in the distribution of f uorescently labeled p-c-Jun were automatically analyzed and quantif ed using image-based algorithms and exported to an Excel spreadsheet. An average of 90 cells per f eld and a total of 10 f elds per well were counted. Each data point is the average of three wells displayed as the total nuclear f uorescence (determined by colocalization with Hoechst 33342) plus the total cytoplasmic f uorescence.

Statistics

Unless otherwise indicated, all results are displayed as means ± SD of triplicates. PGE_2 data are displayed as means of duplicates ± SD (range). Only data from experiments conf rmed at least once are displayed. When compound potencies were compared, data for the same experiment in the same cell preparation are shown. One-way ANOVA, followed by the Tukey-Kramer test, was used for statistical evaluation. (*, $p < 0.05$; **, $p < 0.01$).

Results

CEP-1347 and CEP-11004 as inhibitors of astrocyte NO release

A CCM, a mixture of the proinf ammatory cytokines IL-1β, TNF-α and IFN-γ, was used to induce a fulminant inf ammatory state in murine astrocytes leading to a robust production of NO, PGs, and cytokines (1).

In this model, two MLK inhibitors, CEP-1347 and CEP-11004, were f rst tested for their effect on NO release as a simple general measure of astrocyte activation. CEP-1347 and CEP-11004 both

completely abolished the NO production in astrocytes at concentrations >500 nM. The IC_{50} values were 90 ± 10 nM for CEP-1347 and 251 ± 19 nM for CEP-11004 (Fig. 1*A*). To rank the potency of compounds within our model, we compared the MLK inhibitors to established anti-inf ammatory tool compounds. Ono-2506 is a novel inhibitor reported to reduce astrocyte inf ammation in vivo and is the only known astrocyte-specif c compound (24). This drug reduced the production of NO in a concentration-dependent fashion although with 1,000 times less potency compared with MLK inhibitors (Fig. 1*B*). Both JNK and p38 inhibition reduced the production of NO. However, complete inhibition as seen with CEP-1347 and 11004 was not observed at concentrations up to 5 μM of SP60125 and SB203580 (Fig. 1*C*). MLKs have been reported to reside upstream of both JNK and p38. Therefore, we tested whether inhibition of p38 (by SB203580) and JNK (by SP600125) together could explain the complete abolishment of NO production by the MLK inhibitors. The two stress-activated protein kinase inhibitors showed a clearly additive effect and combination treatment resulted in almost full inhibition of NO production when both compounds were used at 5 μM (Fig. 1*D*).

Effect of MLK inhibitors on the induction of inflammator enzymes

To examine whether the inhibition of NO production may be due to direct iNOS inhibition, we stimulated the cells for 16 h, washed the cytokines away, and added CEP-1347 with or without cycloheximide. Under these conditions, iNOS is already induced when the drug is added, and a potential inhibition of the steady state production was examined. Our results showed that CEP-1347 is not a direct iNOS inhibitor (no block of steady state production) and also that most of the iNOS enzyme had already been produced at 16 h (no difference whether cycloheximide was added or not) (Fig. 2*A*).

Next, we examined whether the effect of CEP-1347 was rather explained by blockage of iNOS protein expression. Western blot analysis showed that up-regulation of iNOS was clearly prevented by MLK, JNK, and p38 inhibition. The general marker for activated astrocytes, GFAP, was not affected by the inhibitors (Fig. 2*B*). Expression of another inf ammation-specif c protein, Cox-2, was also blocked similarly to iNOS.

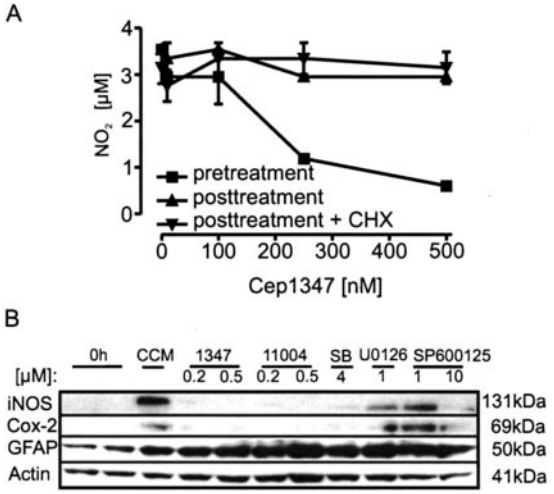

FIGURE 2. MLK inhibitors selectively block expression of inf ammatory proteins. *A*, Cells were treated with CCM for 16 h, washed twice, and further incubated in fresh medium without cytokines. CEP-1347, with or without the protein synthesis inhibitor cycloheximide (CHX, 10 μM), was added to the cells and after 6 h, newly produced nitrite was measured. Cells pretreated with CEP-1347 during the 16 h iNOS induction phase served as a positive control for the effect of the MLK inhibitor. Data are displayed as means of triplicates ± SD. *B*, Cells were pretreated for 30 min with MLK, ERK, JNK, or p38 inhibitors and treated for 24 h with CCM. Western blot analysis was performed on astrocyte lysates using Abs against iNOS, Cox-2, GFAP, and β-actin.

CEP-1347 and CEP-11004 as general inhibitors of astrocyte inflammatio

After these f ndings of a potential anti-inf ammatory effect, the MLK inhibitors were tested for their ability to also prevent cytokine and PG production in the model. Both inhibitors down-regulated the production of IL-6 and PGE_2, similarly potent as NO. This suggests that the MLK inhibitors worked as more general blockers of astrocyte activation (Fig. 3, *A* and *B*). Removal of IFN

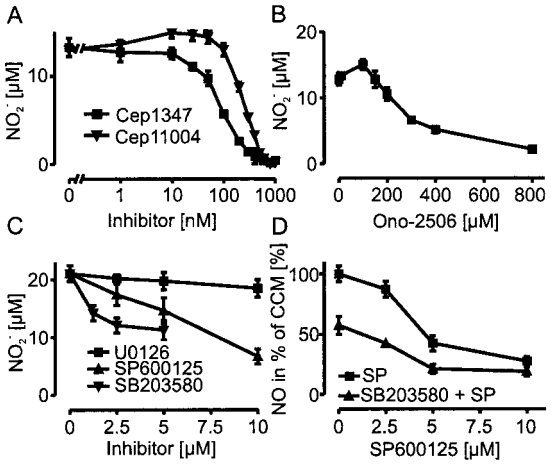

FIGURE 1. Inhibition of NO release from activated astrocytes by CEP-1347 and reference compounds. Primary astrocytes were pretreated for 30 min with: *A*, the MLK inhibitors CEP-1347 or CEP-11004; *B*, Ono-2506; *C*, inhibitors of the ERK (U0126), JNK (SP600125), and p38 (SB203580) pathways; or *D*, inhibitors of JNK (SP = SP600125) and p38 (SB203580, 5 μM) together. CCM was added, the incubation continued for 24 h, supernatants were harvested and examined for nitrite. Data are displayed as means ± SD of triplicate determinations.

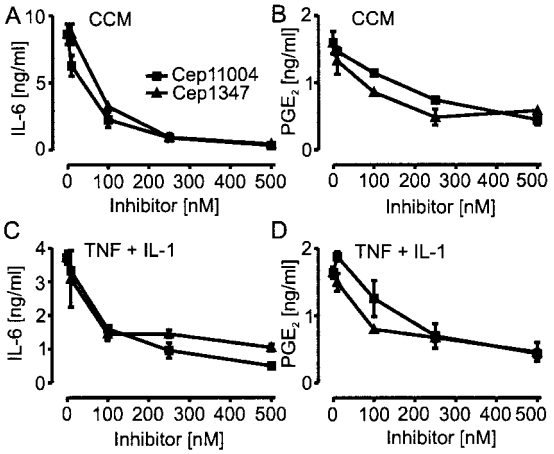

FIGURE 3. Effects of MLK inhibitors on cytokine-driven inf ammation. Cells were pretreated for 30 min with the MLK inhibitors CEP-1347 or CEP-11004. Then CCM (*A* and *B*) or TNF-α (10 ng/ml) plus IL-1β (10 ng/ml) (*C* and *D*) were added for 24 h. Supernatants were harvested after 24 h and examined for IL-6 (*A* and *C*) or PGE_2 (*B* and *D*). Data are displayed as means of triplicates ± SD for IL-6 and as means ± range (n = 2) for PGE_2.

from the cytokine mix used to activate the cells abolished the production of NO, reduced the production of IL-6, but did not affect the production of PGE_2. This change of the stimulation condition did not affect the inhibitory properties and potency of the drugs (Fig. 3, *C* and *D*). The effect of the Ono-2506 and MAPK inhibitors was also tested against IL-6 production. Ono-2506 showed the same low potency/high efficacy as for NO (Fig. 4). All MAPK inhibitors had a larger effect on IL-6 production than on NO, suggesting a selective regulation of different pathways (Fig. 4*B*). Nevertheless, the MLK inhibitors were at least one order of magnitude more potent.

CEP-1347 and CEP-11004 act on their expected target pathway in primary astrocytes

We examined whether MAPK pathways were activated and modified as expected. CCM induced a long-lasting, strong activation of ERK and JNK, peaking at 1 h and staying up for at least 4 h for ERK and 8 h for JNK (Fig. 5*A*). After 1 h stimulation, ERK and JNK phosphorylation were up-regulated 27 and 8 times, respectively, as determined by densitometric scans of triplicate determinations (not shown). We selected the 1 h time point for additional experiments, and observed an increased phosphorylation of c-Jun (a downstream transcription factor of JNK). Moreover, phosphorylation of MKK3/6, an upstream kinase of p38, was increased (Fig. 5, *B* and *C*).

MLK inhibition reduced the phosphorylation of JNK and c-Jun (Fig. 5*B*). Quantitation of JNK phosphorylation by immunoblot densitometry confirmed a significant ($p < 0.01$) inhibition by 60 ± 7%. To complement the immunoblot analysis, we used a single cell immunofluorescence approach to quantify the effect of CEP-1347 and SP600125 on c-Jun phosphorylation, the terminal event of the JNK signaling chain. An accumulation of phosphorylated c-Jun was observed within the nucleus, but an even stronger staining was observed in the cytoplasm of activated cells in structures resembling cytoskeletal elements (Fig. 6*A*). This staining was increased significantly as early as 15 min after cytokine treatment, peaked at 60 min, and decreased again after 4 h (Fig. 6*B*). We again selected the 1 h time point for additional experiments, and observed a complete inhibition of c-Jun phosphorylation by pretreatment with 200 nM CEP-1347. SP600125 prevented c-Jun phosphorylation partially at the concentrations used in this study (Fig. 6*C*).

The band for p-MKK3/6, the upstream kinases of p38, was also reduced by MLK inhibition (Fig. 5*C*) suggesting that MLK inhibition affects signaling by inhibiting activation of both the JNK and the p38 pathways. No significant effects were seen for MLK inhibitor treatment on AKT_{Ser473} phosphorylation or ERK (data not shown). Inhibitors of p38 (SB203580) and MEK1 (U0126) had

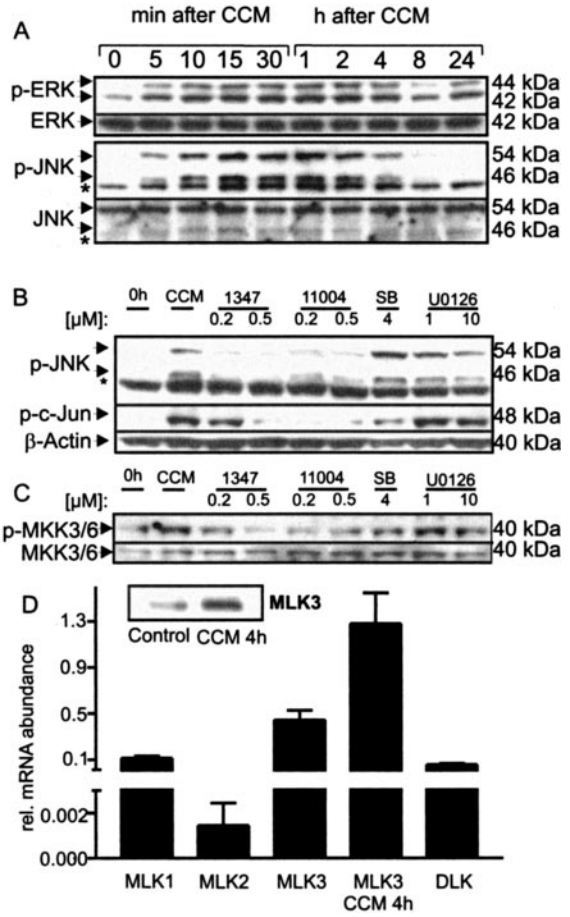

FIGURE 5. Modulation of astrocyte MAPK signaling by MLK inhibitors and reference compounds. Cells were treated with CCM and probed for kinase activation by Western blot analysis with phosphorylation state-specific Abs. *A*, Cells were lysed after the times indicated. After blotting with the phosphospecific Abs, the membranes were stripped and reprobed with Abs for total kinase amount. *, Unspecific, constitutively present band. *B*, The effect of MLK, ERK, and p38 inhibitors on the JNK pathway was examined. Cells were pretreated with inhibitors for 30 min. Cells were lysed 1 h after CCM addition. β-Actin was used as a loading control. *C*, The samples of *B* were analyzed for p-MKK3/6 (upstream kinases of the p38 MAPK pathway). The membranes were reprobed with pan-MKK3/6 Abs. *D*, Total RNA was purified from untreated cells or cells treated with CCM for 4 h, and reverse transcribed to cDNA. Differences in mRNA expression were determined by quantitative PCR and data presented as relative levels normalized to the GAPDH concentration in the sample. All data are presented as means of triplicates ± SD. *Inset*, Cells were treated with CCM for 4 h. Western blot analysis was performed on astrocyte lysates using Abs against MLK3.

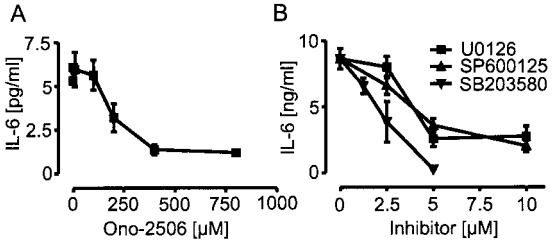

FIGURE 4. Effect of reference inflammation inhibitors on CCM-triggered IL-6 production of astrocytes. Primary astrocytes were pretreated for 30 min with: *A*, Ono-2506; *B*, inhibitors of the ERK (U0126), JNK (SP600125), and p38 (SB203580) pathways. CCM was added and the incubation continued for 24 h. Supernatants were harvested and examined for IL-6. Data are displayed as means ± SD for triplicate determinations

no significant effect on the phosphorylation state of any of the kinases examined. Because this is the first report describing a role of the MLK family in astrocytes, we examined the expression of the different MLK family members. MLK 1, 3, and DLK were all highly expressed, while MLK 2 was expressed at a lower level (Fig. 5*D*). An interesting observation is that MLK3 expression was enhanced by cytokine treatment, both on the mRNA and the protein level (Fig. 5*D*).

Effect of CEP-1347 and CEP-11004 on NF-κB activation

NF-κB is one of the master controllers of inflammation. Its activation is associated with cytoplasm-to-nucleus translocation. Therefore, we used NF-κB translocation from the cell cytosol to the nucleus as a measure of NF-κB activation. This change in

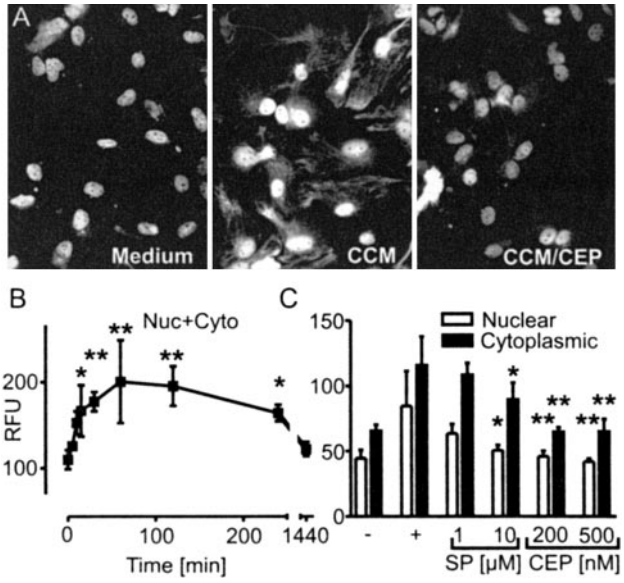

FIGURE 6. CEP-1347 blocks phosphorylation of c-Jun. Cells were treated with CCM and probed for c-Jun activation by immunocytochemistry with a phosphorylation state-specif c Ab. *A*, Pictures representative of the quantif ed image material are presented for untreated cells or cells stimulated with CCM ± CEP. *B*, A time course of c-Jun phosphorylation. Cells were f xed and stained at different times after CCM addition. Phosphorylation of c-Jun was quantif ed in the nucleus and in the perinuclear region of astrocytes. Data are the means of triplicates ± SD (at least 300 cells/well were analyzed) and are presented as relative f uorescent units (RFU) (nuclear plus perinuclear f uorescence). *C*, Cells were pretreated with CEP-1347 or SP600125 for 30 min. Cells were f xed and stained 1 h after CCM addition. Phosphorylation of c-Jun was quantif ed in the nucleus or in the perinuclear region of astrocytes. Data are the means of triplicates ± SD (at least 300 cells/well were analyzed) and are presented as RFU measured in the nucleus or in the cytoplasm (perinuclear).

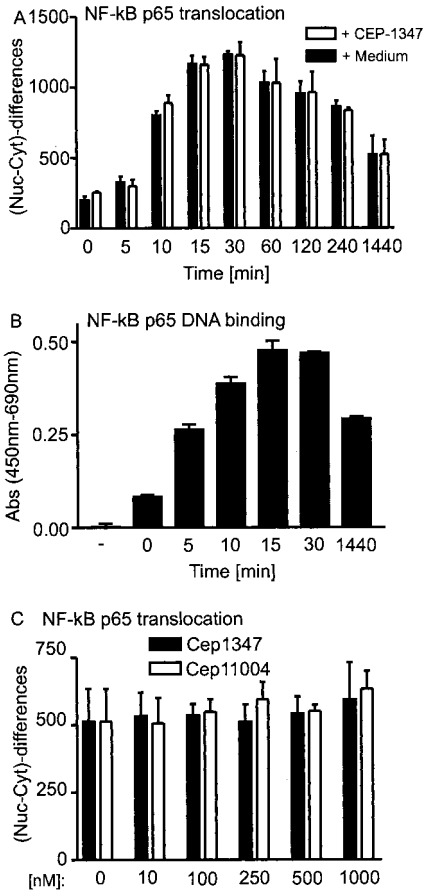

FIGURE 7. No effect of MLK inhibitors on NF-κB translocation. *A*, Primary astrocytes were treated for different periods of time with CCM ± CEP-1347 (500 nM), f xed, and stained for the p65 subunit of NF-κB. Data are presented as the total nuclear-cytoplasmic intensity ratio (arbitrary units). *B*, Cells were treated for different times with CCM and lysed. The cell lysate was assessed for NF-κB activity by an ELISA method. *C*, Cells were pretreated for 30 min with various concentrations of CEP-1347 or CEP-11004 and the NF-κB translocation assay was performed. All data are presented as means of triplicates ± SD.

cellular localization was assessed by quantitative immunocytochemistry. A large translocation of NF-κB was seen already after 5 min of stimulation with CCM, with a maximal amount of NF-κB being in the nucleus 15–30 min after CCM addition. The amount of NF-κB within the nucleus decreased gradually over 24 h (Fig. 7*A*). The data from the translocation assay correlated well with data from an NF-κB DNA binding assay (Fig. 7*B*), showing that the translocation assay is suitable for the assessment of NF-κB activation. To evaluate the effect of MLK inhibition on NF-κB activation, we added MLK inhibitors before stimulating cells for various times with CCM. Two different MLK inhibitors did not affect NF-κB translocation at any time point (Fig. 7, *A* and *C*), suggesting that MLK inhibition in astrocytes reduces inf ammation independently of NF-κB activation.

Effect on transcriptional regulation

Proinf ammatory cytokines trigger a large and complex inf ammatory response in astrocytes. To get further insight into how CEP-1347 modulates this response, we took advantage of a small custom-spotted array containing probes for a representative set of inf ammatory genes known to be activated by CCM. The inf ammation-linked genes chosen were all conf rmed to be regulated by CCM in our model. Total RNA was purif ed from astrocytes stimulated for 4 h under different conditions, and expression levels of relevant pairs of samples were directly compared by hybridization. Our results clearly showed that CEP-1347 was a transcriptional regulator, however, it did not induce a general inhibition of all inf ammation-related genes but differentially modulated the response to CCM treatment. Three types of regulation by CEP-1347 were observed. First, IL-6, iNOS, and Cox-2 were all down-regulated by treatment with the MLK inhibitor, as was granulocyte/macrophage-CSF (GM-CSF), a microglia activation factor (Fig. 8). Second, CEP-1347 treatment did not affect the up-regulation of GSK-3, NF-κB1, CD95, caspase 11, and manganese superoxide dismutase (MnSOD). Third, two genes that were induced by CCM treatment (one borderline) were even further induced by CEP-1347 treatment. Interestingly, these genes were IAP-2, which codes for an antiapoptotic protein, and ATF4, a transcription factor involved in a general antioxidant response (Fig. 8). The latter gene was also induced after treatment of control astrocytes by CEP-1347 alone (Fig. 9*H*).

To conf rm the differential hybridization data, we performed quantitative PCR both looking at the 4 and 8 h time point. Cox-2, iNOS, and IL-6 mRNA were down-regulated by CEP-1347 treatment at both time points (Fig. 9, *A–C*). Two genes, which were not represented on the hybridization array, were TNF-α and uPA, an extracellular protease. Both genes were signif cantly down-regulated (Fig. 9, *D* and *E*). The level of RANTES mRNA was reduced slightly at 4 h, conf rming the borderline regulation seen on the array (ratio 0.58), but even more so at 8 h (Fig. 9*G*). At 4 h, IAP-2 and ATF4 were both signif cantly up-regulated by CEP-1347/

FIGURE 8. The anti-inf ammatory prof le of CEP-1347. Cells were pretreated for 30 min with CEP-1347 before treatment for 4 h with CCM. Total RNA was purif ed and labeled cDNA was prepared. Different competitive cDNA hybridization experiments were done on a small custom array for CCM vs control, CCM + CEP-1347 (500 nM) vs control and CCM + CEP-1347 vs CCM. Data presented are the average of two dye-swap hybridizations for one cell preparation. All data are presented as means of duplicates ± range.

	Fold induction			
Gene name/product	CCM Vs CTR	CCM+CEP Vs CTR	CCM+Cep Vs CCM	Genbank
activating transcription factor 4, atf4	1.9 ± 0.5	2.1 ± 0.8	2.3 ± 0.3	NM_001675
Birc2, baculoviral IAP repeat-containing 2	10.0 ± 4.0	13.5 ± 6.3	2.3 ± 0.1	NM_007464
B2m, beta-2 microglobulin	3.1 ± 1.0	2.9 ± 1.0	1.4 ± 0.2	NM_009735
Caspase 11	7.2 ± 7.3	7.9 ± 1.8	1.4 ± 0.1	NM_007609
FAS, Tnfrsf6, CD95	4.1 ± 0.2	3.4 ± 0.2	1.1 ± 0.1	NM_007987
M-CSF, colony stimulating factor 1	3.2 ± 0.1	3.4 ± 1.2	1.1 ± 0.0	NM_007778
GSK3, glycogen synthase kinase 3	2.8 ± 0.8	2.7 ± 0.5	1.0 ± 0.3	XM_133269
NF-kappaB1,	7.1 ± 2.8	4.6 ± 1.3	1.0 ± 0.3	NM_008689
MnSOD, superoxide dismutase 2	4.9 ± 0.2	5.9 ± 0.2	1.0 ± 0.2	NM_013671
MCP-1, Scya2, CCL2	77.9 ± 55.4	53.5 ± 25.0	0.7 ± 0.3	NM_011333
RANTES, Scya5, CCL5	8.1 ± 1.7	15.5 ± 11.4	0.6 ± 0.1	NM_013653
IL6, interleukin 6	14.4 ± 14.6	3.0 ± 1.1	0.4 ± 0.1	NM_031168
GM-CSF, colony stimulating factor 2	10.0 ± 7.9	2.4 ± 0.1	0.4 ± 0.0	XM_109951
Nos2, iNOS	10.0 ± 2.2	2.1 ± 0.4	0.4 ± 0.0	NM_010927
Cox-2, prostaglandin-endoperoxide syn. 2	6.0 ± 1.9	2.4 ± 0.4	0.4 ± 0.1	NM_011198

CCM compared with CCM treatment, but at 8 h CEP-1347 affected neither gene (Fig. 9, *F* and *H*). Thus, PCR data fully confirmed and further complemented the hybridization data.

Effects of delayed drug treatment

To obtain some preliminary information on whether CEP-1347 only blocks the onset of inf ammation or may also be effective in dampening it, once initiated, we added CEP-1347 at different time points after CCM. Expression of iNOS and Cox-2 was then quantif ed 8 h after CCM stimulation. CEP-1347 entirely blocked iNOS regulation when given up to 4 h after CCM and reduced the mRNA for iNOS by 50% when given after 6 h. At these time offsets, Cox-2 regulation was still entirely blocked (Fig. 10, *A* and *C*). This probably ref ects the different half-lives of the two mRNAs, but also shows that CEP-1347 does not have to be present before the insult, but can interrupt astrocytic reactivity even when administered at a later stage of inf ammation. Furthermore, it also suggests a continued MLK activation in our model. The PCR data for iNOS were conf rmed by nitrite measurements done after 24 h of CCM treatment. When CEP-1347 was added 6 h post-CCM it prevented ~50% of the NO produced after 24 h (Fig. 10*B*).

Discussion

The pan-MLK inhibitor CEP-1347 is neuroprotective in many different disease models in vitro and in vivo (29–32). Up to now all studies on the ability of CEP-1347 to block neurodegeneration were focused on direct neuroprotection, while any possible effects on glial cells have been neglected. In this study, we show, for the f rst time that CEP-1347 also acts on astrocytes, and we provide evidence for MLK kinases as pivotal drivers in astrocytic inf ammation.

Astrocytes are the most abundant cell type in the brain (comprising up 50–60% of the total cell number) and the position surrounding the blood-brain barrier makes astrocytes important regulators of cell traff cking into the brain (2, 33). Like Kupffer cells in the liver, astrocytes have a sentinel function and are capable of launching a powerful innate immune response to battle infection and shield off areas of damage. This astrocytic immune response can become overly activated after damage to the brain, and this can further exacerbate neurodegenerative processes.

In inf ammatory settings, astrocytes cooperate with microglia, which provide the f rst wave of inf ammatory cytokines. Therefore,

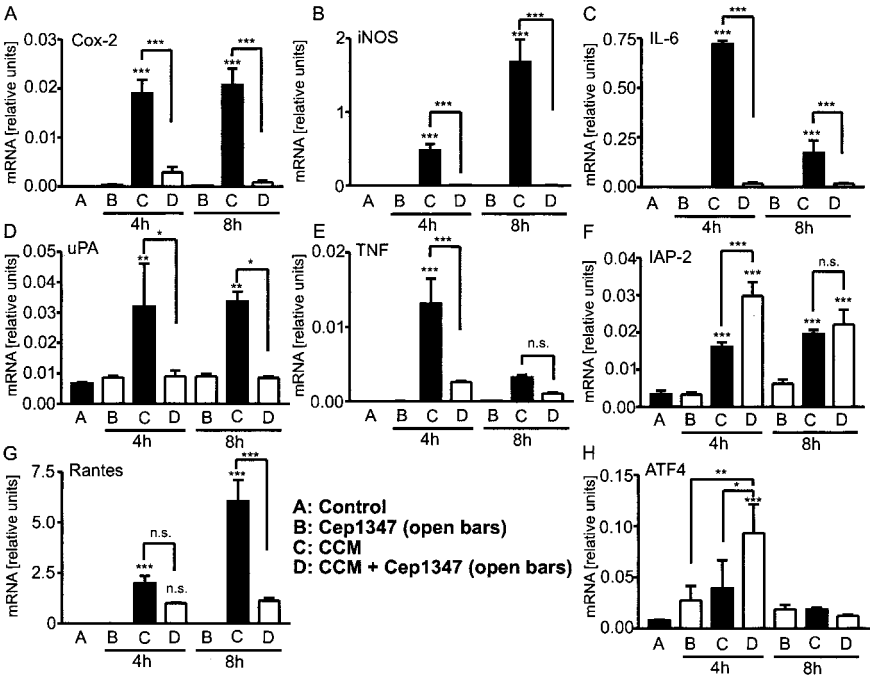

FIGURE 9. Quantitative PCR measurements of inf ammation-related RNAs. Cells were pretreated for 30 min with CEP-1347 (500 nM) and treated with CCM for 4 or 8 h. Total RNA was purif ed and reverse transcribed to cDNA. Differences in mRNA expression were determined by quantitative PCR and data presented as relative levels normalized to the GAPDH concentration in the sample. All data are presented as means of triplicates ± SD.

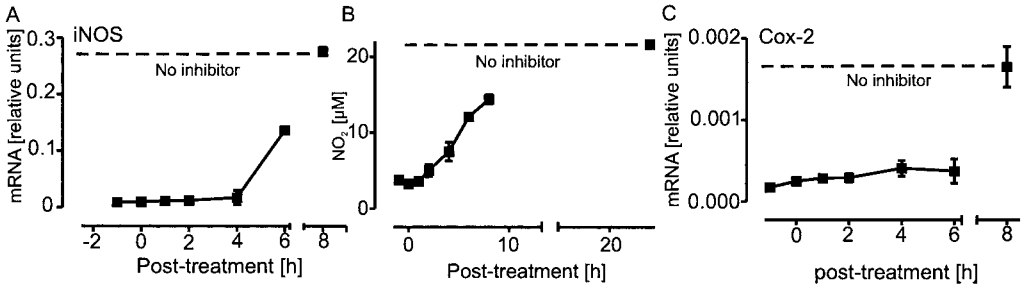

FIGURE 10. Reversal of initiated inf ammation by treatment with CEP-1347. *A*, Astrocytes were treated with CCM for 8 h (all data points) and CEP-1347 (500 nM) was added at different times as indicated on the *x*-axis. After the end of the experiment, total RNA was purif ed and reverse transcribed. Quantitative PCR measurements of iNOS transcripts were performed and are displayed as GAPDH-normalized values. *B*, Cells were treated with CCM for 24 h and CEP-1347 (500 nM) was added at different times as indicated on the *x*-axis. NO production was measured 24 h after CCM addition. *C*, Cox-2 transcripts were quantif ed from the same cDNA preparations as in *A*. All data are presented as means of triplicates ± SD.

we used a model where primary astrocytes were stimulated by a mixture of such microglia-derived factors. In this set-up, we f rst tested two inhibitors of the mixed lineage kinase (MAPKKK) family, CEP-1347 and CEP-11004, for their ability to inhibit NO production and we found that they had surprisingly strong anti-inf ammatory effects (100% inhibition) within the normal concentration known for MLK inhibition. Their effect was not due to direct inhibition of iNOS, but due to prevention of the transcription of the enzyme as indicated by the results from the hybridization experiment and conf rmed by PCR. One aspect of the ability of CEP-1347 to block astrocyte activation, requiring more attention in the future, was the ability of the drug to stop an already ongoing immune response. This could make the drug highly interesting for chronic disease situations.

MLK inhibitors have not previously been tested on astrocytes. Therefore, we investigated whether their effects correlated with the known inhibitory activity of CEP-1347 on MAPK pathways. By use of p-MAPK-specif c Abs and various inhibitors, we established initially that cytokine stimulation indeed activates the relevant kinases. Then we conf rmed that specif c p38 and JNK inhibitors both reduced the production of the various inf ammatory mediators. In agreement with the upstream position of MLKs to p38 and JNK, we observed that p38 and JNK inhibitors resulted in a similar extent of inhibition as CEP-1347 only when used in combination. Despite the clear effect of various highly specif c p38 inhibitors in our astrocyte model system (3), we were not successful in measuring p38 phosphorylation in astrocytes directly. We do not know the reason for this, because the technology worked well in our laboratory on other cell types. As a surrogate, we measured phosphorylation of MKK3/6, the kinase directly upstream of p38. Together, our results suggest that CEP1347 indeed modulates the inf ammation-associated activity of stress-activated kinases. Thus, the activity pattern is as expected and f rmly established in other cellular systems (15, 22). Moreover, recent unpublished data from our laboratory indicate that a regulation of JNK and of p38 signaling by CEP1347 also occurs in activated microglia cells. In contrast, we did not observe activation of AKT or ERK in astrocytes following CEP-1347 treatment, as has been reported for neurons by one group (34), suggesting that the induced upstream block of the p38 and JNK pathway appears to be the most likely mechanism of the effects of CEP-1347.

As in other inf ammatory cells, NF-κB was activated strongly in astrocytes, and MLK3 has been reported to affect NF-κB activation (35). NF-κB is an important regulator of inf ammatory signaling, but it has also been implicated in cellular survival and in antioxidative defense. Thus, a strong inhibition of NF-κB may have unwanted side effects in neurodegenerative conditions (36, 37). We found that CEP-1347 treatment did not affect NF-κB activation in our system and this f ts with other group's observations that MLK3 can affect NF-κB activity under certain conditions, but not after proinf ammatory cytokine treatment (38). Independent support for this notion was provided by the array experiment. Multiple NF-κB-regulated genes were examined (for a review, see Ref. 37), and the lack of regulation of these genes by CEP-1347 is in agreement with our results from the translocation assay, which demonstrates that CEP-1347 does not block NF-κB signaling.

From our initial results it could appear that CEP-1347 would block the up-regulation of all inf ammatory genes, unspecif cally. To test this, we hybridized cDNA from various combinations of CCM and CEP-1347-treated samples onto a small custom spotted array. From this experiment, it was apparent that CEP-1347 did not block transcription of all inf ammation-regulated genes, but only a specif c subset: iNOS, IL-6, Cox-2, GM-CSF, RANTES (borderline). Although many genes were not affected signif cantly (ex., MnSOD), other genes were even up-regulated (ATF4, IAP-2). This showed that CEP-1347 worked as a differential modulator of astroglial inf ammation and not only as a strictly anti-inf ammatory drug. Results from the array were fully conf rmed by quantitative PCR and we further observed a down-regulation of TNF and uPA, two genes not present in the hybridization experiment.

IAP-2 is a member of an antiapoptotic family of proteins directly responsible for caspase inhibition (39, 40). Inf ammation can render astrocytes sensitive to apoptosis induction, e.g., via the Fas system, and CEP-1347 may act antiapoptotic and protective by up-regulation of IAP-2. Another factor possibly contributing to astrocyte survival under inf ammatory conditions is ATF4. This transcription factor (also called CREB-2, TAXREB67, or C/ATF) is responsible for cell survival during episodes of metabolic or oxidative stress (41, 42). ATF4 is an important regulator of amino acid transporters and proteins involved in antioxidative stress responses (42). The antioxidant glutathione is essential for the cellular detoxif cation of reactive oxygen species in the brain and astrocytes are the only cell type capable of exporting glutathione to the extracellular milieu and to neurons (43). This may be of relevance during episodes of inf ammation or tissue injury when enormous amounts of reactive oxygen species are generated. Notably, CEP-1347 did not affect the benef cial inf ammation-induced up-regulation of MnSOD, an enzyme that scavenges superoxide and converts it to hydrogen peroxide. For the disposal of hydrogen peroxide, cells require glutathione. Thus, the balanced regulation of SOD and ATF4 by CEP-1347 provides astrocytes with a good basis to f ght oxidative stress during inf ammation.

In conclusion, we report here initial evidence that the MLKs are involved in astrocyte inf ammatory signaling. Furthermore, we

show that the neuroprotective MLK inhibitor CEP-1347 has a complex and specif c anti-inf ammatory prof le, reducing cytokine/chemokine production while at the same time inducing an anti-apoptotic and antioxidative response in primary cultures of astrocytes. There is a possibility that MLK inhibitors may have potential as anti-inf ammatory agents. However, further work on non-neuronal cell types and in vivo models is required to corroborate this hypothesis.

Acknowledgments

We gratefully acknowledge the excellent technical assistance and input of Andreas Rassov, Søren Lund, and Trine Marie Nielsen. We are furthermore indebted to Drs. Kenneth Thirstrup and Jan Egebjerg for valuable contributions and insightful discussions during the course of this work and to Lise Silbye for proofreading.

References

1. Eddleston, M., and L. Mucke. 1993. Molecular prof le of reactive astrocytes–implications for their role in neurologic disease. *J. Neurosci. 54:15.*
2. Dong, Y., and E. N. Benveniste. 2001. Immune function of astrocytes. *Glia 36:180.*
3. Falsig, J., M. Latta, and M. Leist. 2004. Def ned inf ammatory states in astrocytes: correlation with susceptibility towards CD95-driven apoptosis. *J. Neurochem. 88:181.*
4. Hensley, K., R. A. Floyd, N. Y. Zheng, R. Nael, K. A. Robinson, X. Nguyen, Q. N. Pye, C. A. Stewart, J. Geddes, W. R. Markesbery, et al. 1999. p38 kinase is activated in the Alzheimer's disease brain. *J. Neurochem. 72:2053.*
5. Ferrer, I., R. Blanco, M. Carmona, B. Puig, M. Barrachina, C. Gomez, and S. Ambrosio. 2001. Active, phosphorylation-dependent mitogen-activated protein kinase (MAPK/ERK), stress-activated protein kinase/c-Jun N-terminal kinase (SAPK/JNK), and p38 kinase expression in Parkinson's disease and dementia with Lewy bodies. *J. Neural Transm. 108:1383.*
6. Piao, C. S., Y. Che, P. L. Han, and J. K. Lee. 2002. Delayed and differential induction of p38 MAPK isoforms in microglia and astrocytes in the brain after transient global ischemia. *Brain Res. Mol. Brain Res. 107:137.*
7. Ferrer, I., P. Pastor, M. J. Rey, E. Munoz, B. Puig, E. Pastor, R. Oliva, and E. Tolosa. 2003. τ phosphorylation and kinase activation in familial tauopathy linked to deln296 mutation. *Neuropathol. Appl. Neurobiol. 29:23.*
8. Ferrer, I., M. Barrachina, M. Tolnay, M. J. Rey, N. Vidal, M. Carmona, R. Blanco, and B. Puig. 2003. Phosphorylated protein kinases associated with neuronal and glial τ deposits in argyrophilic grain disease. *Brain Pathol. 13:62.*
9. Shin, T., M. Ahn, K. Jung, S. Heo, D. Kim, Y. Jee, Y. K. Lim, and E. J. Yeo. 2003. Activation of mitogen-activated protein kinases in experimental autoimmune encephalomyelitis. *J. Neuroimmunol. 140:118.*
10. Migheli, A., R. Piva, C. Atzori, D. Troost, and D. Schiffer. 1997. c-Jun, JNK/SAPK kinases and transcription factor NF-κB are selectively activated in astrocytes, but not motor neurons, in amyotrophic lateral sclerosis. *J. Neuropathol. Exp. Neurol. 56:1314.*
11. Hua, L. L., M. L. Zhao, M. Cosenza, M. O. Kim, H. Huang, H. B. Tanowitz, C. F. Brosnan, and S. C. Lee. 2002. Role of mitogen-activated protein kinases in inducible nitric oxide synthase and TNFα expression in human fetal astrocytes. *J. Neuroimmunol. 126:180.*
12. Harper, S. J., and N. Wilkie. 2003. MAPKs: new targets for neurodegeneration. *Expert Opin. Ther. Targets 7:187.*
13. Barone, F. C., E. A. Irving, A. M. Ray, J. C. Lee, S. Kassis, S. Kumar, A. M. Badger, J. J. Legos, J. A. Erhardt, E. H. Ohlstein, et al. 2001. Inhibition of p38 mitogen-activated protein kinase provides neuroprotection in cerebral focal ischemia. *Med. Res. Rev. 21:129.*
14. Kikuchi, M., L. Tenneti, and S. A. Lipton. 2000. Role of p38 mitogen-activated protein kinase in axotomy-induced apoptosis of rat retinal ganglion cells. *J. Neurosci. 20:5037.*
15. Gallo, K. A., and G. L. Johnson. 2002. Mixed-lineage kinase control of JNK and p38 MAPK pathways. *Nat. Rev. Mol. Cell Biol. 3:663.*
16. Vacratsis, P. O., and K. A. Gallo. 2000. Zipper-mediated oligomerization of the mixed lineage kinase SPRK/MLK-3 is not required for its activation by the GTPase cdc 42 but is necessary for its activation of the JNK pathway: monomeric SPRK L410P does not catalyze the activating phosphorylation of Thr^{258} of murine mitogen-activated protein kinase kinase 4. *J. Biol. Chem. 275:27893.*
17. Yasuda, J., A. J. Whitmarsh, J. Cavanagh, M. Sharma, and R. J. Davis. 1999. The JIP group of mitogen-activated protein kinase scaffold proteins. *Mol. Cell. Biol. 19:7245.*
18. Kelkar, N., S. Gupta, M. Dickens, and R. J. Davis. 2000. Interaction of a mitogen-activated protein kinase signaling module with the neuronal protein JIP3. *Mol. Cell. Biol. 20:1030.*
19. Xu, Z., N. V. Kukekov, and L. A. Greene. 2003. POSH acts as a scaffold for a multiprotein complex that mediates JNK activation in apoptosis. *EMBO J. 22:252.*
20. Buchsbaum, R. J., B. A. Connolly, and L. A. Feig. 2002. Interaction of Rac exchange factors Tiam1 and Ras-GRF1 with a scaffold for the p38 mitogen-activated protein kinase cascade. *Mol. Biol. Cell 22:4073.*
21. Kaneko, M., Y. Saito, H. Saito, T. Matsumoto, Y. Matsuda, J. L. Vaught, C. A. Dionne, T. S. Angeles, M. A. Glicksman, N. T. Neff, et al. 1997. Neurotrophic 3,9-bis[(alkylthio)methyl]-and-bis(alkoxymethyl)-K-252a derivatives. *J. Med. Chem. 40:1863.*
22. Maroney, A. C., J. P. Finn, T. J. Connors, J. T. Durkin, T. Angeles, G. Gessner, Z. Xu, S. L. Meyer, M. J. Savage, L. A. Greene, et al. 2001. Cep-1347 (KT7515), a semisynthetic inhibitor of the mixed lineage kinase family. *J. Biol. Chem. 276:25302.*
23. Murakata, C., M. Kaneko, G. Gessner, T. S. Angeles, M. A. Ator, T. M. O'Kane, B. A. McKenna, B. A. Thomas, J. R. Mathiasen, M. S. Saporito, et al. 2002. Mixed lineage kinase activity of indolocarbazole analogues. *Bioorg. Med. Chem. Lett. 12:147.*
24. Tateishi, N., T. Mori, Y. Kagamiishi, S. Satoh, N. Katsube, E. Morikawa, T. Morimoto, T. Matsui, and T. Asano. 2002. Astrocytic activation and delayed infarct expansion after permanent focal ischemia in rats. II. Suppression of astrocytic activation by a novel agent (R)-(-)-2-propyloctanoic acid (ONO-2506) leads to mitigation of delayed infarct expansion and early improvement of neurologic def cits. *J. Cereb. Blood Flow Metab. 22:723.*
25. Weinstein, D. E. 1997. Isolation and purif cation of primary rodent astrocytes. In *Current Protocols in Neuroscience*. Wiley, p. 3.5.1.
26. Hughes, T. R., M. Mao, A. R. Jones, J. Burchard, M. J. Marton, K. W. Shannon, S. M. Lefkowitz, M. Ziman, J. M. Schelter, M. R. Meyer, et al. 2001. Expression prof ling using microarrays fabricated by an ink-jet oligonucleotide synthesizer. *Nat. Biotechnol. 19:342.*
27. Knudsen, S. *A Biologist's Guide to Analysis of cDNA Microarray Data*. 2002. New York, Wiley Interscience.
28. Renard, P., I. Ernest, A. Houbion, M. Art, H. Le Calvez, M. Raes, and J. Remacle. 2001. Development of a sensitive multi-well colorimetric assay for active NFκB. *Nucleic Acids Res. 29:E21.*
29. Maroney, A. C., J. P. Finn, D. Bozyczko-Coyne, T. M. O'Kane, N. T. Neff, A. M. Tolkovsky, D. S. Park, C. Y. Yan, C. M. Troy, and L. A. Greene. 1999. CEP-1347 (KT7515), an inhibitor of JNK activation, rescues sympathetic neurons and neuronally differentiated PC12 cells from death evoked by three distinct insults. *J. Neurochem. 73:1901.*
30. Harris, C., A. C. Maroney, and E. M. Johnson, Jr. 2002. Identif cation of JNK-dependent and -independent components of cerebellar granule neuron apoptosis. *J. Neurochem. 83:992.*
31. Saporito, M. S., E. M. Brown, M. S. Miller, and S. Carswell. 1999. CEP-1347/KT-7515, an inhibitor of c-jun N-terminal kinase activation, attenuates the 1-methyl-4-phenyl tetrahydropyridine-mediated loss of nigrostriatal dopaminergic neurons in vivo. *J. Pharmacol. Exp. Ther. 288:421.*
32. Saporito, M. S., R. L. Hudkins, and A. C. Maroney. 2002. Discovery of CEP-1347/KT-7515, an inhibitor of the JNK/SAPK pathway for the treatment of neurodegenerative diseases. *Prog. Med. Chem. 40:23.*
33. Weiss, J. M., S. A. Downie, W. D. Lyman, and J. W. Berman. 1998. Astrocyte-derived monocyte-chemoattractant protein-1 directs the transmigration of leukocytes across a model of the human blood-brain barrier. *J. Immunol. 161:6896.*
34. Roux, P. P., G. Dorval, M. Boudreau, A. Angers-Loustau, S. J. Morris, J. Makkerh, and P. A. Barker. 2002. K252a and CEP1347 are neuroprotective compounds that inhibit mixed-lineage kinase-3 and induce activation of Akt and ERK. *J. Biol. Chem. 277:49473.*
35. Ng, P. W., H. Iha, Y. Iwanaga, M. Bittner, Y. Chen, Y. Jiang, G. Gooden, J. M. Trent, P. Meltzer, K. T. Jeang, and S. L. Zeichner. 2001. Genome-wide expression changes induced by HTLV-1 Tax: evidence for MLK-3 mixed lineage kinase involvement in Tax-mediated NF-κB activation. *Oncogene 20:4484.*
36. Ghosh, S., and M. Karin. 2002. Missing pieces in the NF-κB puzzle. *Cell 109:S81.*
37. Pahl, H. L. 1999. Activators and target genes of Rel/NF-κB transcription factors. *Oncogene 18:6853.*
38. Hehner, S. P., T. G. Hofmann, A. Ushmorov, O. Dienz, L. Wing-Lan, I., N. Lassam, C. Scheidereit, W. Droge, and M. L. Schmitz. 2000. Mixed-lineage kinase 3 delivers CD3/CD28-derived signals into the IκB kinase complex. *Mol. Cell. Biol. 20:2556.*
39. Salvesen, G. S., and C. S. Duckett. 2002. IAP proteins: blocking the road to death's door. *Nat. Rev. Mol. Cell Biol. 3:401.*
40. Duckett, C. S., F. Li, Y. Wang, K. J. Tomaselli, C. B. Thompson, and R. C. Armstrong. 1998. Human IAP-like protein regulates programmed cell death downstream of Bcl-x_L and cytochrome c. *Mol. Cell. Biol. 18:608.*
41. Hettmann, T., K. Barton, and J. M. Leiden. 2000. Microphthalmia due to p53-mediated apoptosis of anterior lens epithelial cells in mice lacking the CREB-2 transcription factor. *Dev. Biol. 222:110.*
42. Harding, H. P., Y. Zhang, H. Zeng, I. Novoa, P. D. Lu, M. Calfon, N. Sadri, C. Yun, B. Popko, R. Paules, et al. 2003. An integrated stress response regulates amino acid metabolism and resistance to oxidative stress. *Mol. Cell 11:619.*
43. Dringen, R., and J. Hirrlinger. 2003. Glutathione pathways in the brain. *Biol. Chem. 384:505.*